commonest being del(6)(q21–q25) [9]. However, no specific chromosomal translocation has been identified. Iqbal *et al* [10] performed array comparative genomic hybridization on NK-cell malignancies and identified *PRDM1* as the likely target gene in del6q21. Recently, Hwang *et al* [11] performed genome-wide GEP on NKTL and identified overexpression of several genes related to vascular biology, EBV-induced genes, and platelet-derived growth factor receptor α. Deregulation of several oncogenic pathways, such as AKT, STAT3, and nuclear factor-κB pathways, was also detected. Nevertheless, comprehensive genome-wide profiling of NKTL is scarce as extensive research has been limited by the rarity of this entity, the difficulty in obtaining adequate biopsy specimens, extensive tumour necrosis, and the lack of availability of frozen tumour tissue.

Gene expression profiling (GEP) has been extensively used in cancer research in recent years. One major drawback is the requirement for frozen tissue for current methods of genome-wide expression profiling. Recently, Hoshida *et al* demonstrated the feasibility of genome-wide expression profiling of formalin-fixed, paraffin-embedded (FFPE) tissues of hepatocellular carcinoma and identified a molecular signature that correlated with survival [12]. In this study, we performed genome-wide expression profiling on a series of NKTLs using FFPE tissues in relation to normal NK cells and NK tumour cell lines, with the main objective of understanding molecular pathways deregulated in NKTL. In the process, we hope to identify potential new therapeutic targets in a disease where the outcome is poor with current treatment modalities.

Material and methods

Case selection and construction of tissue microarray

Patients with a diagnosis of NKTL were identified from the archives of the Department of Pathology, National University Hospital (NUH), from 1990 to 2009. Additional immunohistochemistry and *in situ* hybridization for EBV-encoded small RNA (EBER) were performed and the cases were classified according to the 2008 WHO lymphoma classification. Cases with no additional tissue available for immunohistochemical or genetic analysis were excluded. A total of 33 cases of NKTL were selected. According to the WHO criteria, all 33 cases expressed CD3, cytotoxic markers (granzyme B and/or TIA-1), and EBER. Immunoreactivity for CD56, CD8, and CD4 was present in 64% (21 cases), 16% (five cases), and 3% (one case), respectively. The clinical and immunophenotypic data of the cases are summarized in the Supporting information, Supplementary Table 1. Tissue microarrays (TMAs) of the 33 cases of NKTL were also constructed (see Supporting information, Supplementary methods).

Nine cases of NKTL with adequate FFPE tissue remaining and good-quality RNA were selected for GEP. In addition, two cases each of normal skin and soft tissue, intestinal, nasal, and lymph node FFPE tissue were also included for GEP analysis as control tissue. The study was approved by the Domain Specific Review Board of the National Healthcare Group, Singapore.

Immunohistochemistry (IHC)

Four-micrometre sections from the TMA blocks were cut for IHC. IHC was performed for c-Myc, p53, survivin, and five NF-κB transcription factors including p50, p52, p65, RelB, and C-Rel (see the Supporting information, Supplementary methods and Supplementary Table 2 for more details). Appropriate positive tissue controls were used.

The immunohistochemical expression for all the antibodies was scored as a percentage of the total tumour cell population per 1 mm core diameter (×400) by one of the authors (NSB). The majority of the cases (97%) had two to four cores represented on the TMA and the final score was obtained as an average of all the individual cores. For c-Myc, p53, and survivin antibodies, positive expression was defined as nuclear staining in 10% or more of the tumour population. For the five NF-κB antibodies (p50, p52, p65, RelB, and C-Rel), only nuclear immunoreactivity was regarded as constitutive NF-κB activation and positive expression was defined as nuclear staining in 10% or more of tumour cells, similar to previous published reports [13].

NK cell lines and cultures

The NK-tumour cell lines used in this study included NK-92 (American Type Culture Collection), KHYG-1 (Japanese Collection of Research Bioresources), HANK-1 (a gift from Dr Y Kagami), SNK-6, SNT-8 (a gift from Dr N Shimizu), and NK-YS (a gift from Dr YL Kwong). Culture conditions are given in the Supporting information, Supplementary methods. The phenotypic and genotypic characteristics of the NK cell lines have been well characterized in previous studies [14,15] and are summarized in the Supporting information, Supplementary Table 3.

Isolation of normal NK cells from peripheral blood

Peripheral blood mononuclear cells (PBMCs) were separated by Ficoll Paque Plus density gradient centrifugation (Amersham Biosciences, Piscataway, NJ, USA) from whole blood samples obtained from healthy donors and buffy coat packs of whole blood samples from the Blood Donation Centre, NUH. Highly pure untouched normal human NK cells were isolated using the NK cell isolation kit (Miltenyi Biotec, Bergisch Gladbach, Germany). The purity of the isolated NK cells as determined by flow cytometry was between 90% and 99%. The isolated NK cells were subsequently stimulated by culturing in the presence of human recombinant IL-2 (Miltenyi Biotec). For cell block preparation, Bouin's solution was added to the

isolated normal NK cell samples, followed by centrifugation. The packed cell sediments were fixed in formalin for tissue processing.

RNA extraction from FFPE, NK cell lines, and normal NK cells

Total RNA from NKTL FFPE tissues and FFPE normal tissue controls was isolated using a High Pure RNA Paraffin Kit (Roche Applied Science, Mannheim, Germany) according to the manufacturer's instructions. All the sections were deparaffinized with xylene, subjected to proteinase K digestion, and RNA was extracted according to the manufacturer's protocol.

Total RNA was extracted from freshly isolated cells from NK cell lines and normal NK cell samples obtained from healthy donors using the miRNeasy Mini Kit (Qiagen GmbH, Hilden, Germany) protocol with DNaseI treatment included. The concentration and purity of the total RNA extracted were measured using a NanoDrop ND 3.0 spectrophotometer (NanoDrop Technologies Inc, Wilmington, DE, USA). RNA quality was assessed with an Agilent 2100 Bioanalyzer (Agilent Technologies, Palo Alto, CA, USA) and an RNA 6000 LabChip Kit (Agilent Technologies). Of the samples with RNA extracted, nine met the quality requirements and were used for GEP and subsequent analysis.

Gene expression profiling and analysis

GEP was performed according to the complementary DNA-mediated annealing, selection, extension, and ligation (DASL) assay (Illumina, Inc, San Diego, CA, USA) [16,17]. Raw signal intensities of each probe were obtained from data analysis software (Beadstudio; Illumina, San Diego, CA, USA). The data were normalized using a linear calibration method. Hierarchical clustering of samples was performed using the Pearson coefficient and the Ward method as the similarity and linkage methods, respectively, using the Bioconductor packages of R. To derive the NKTL-specific gene expression profiles, we extracted genes differentially expressed between NK cell lines and NKTL FFPE samples, and normal NK cells and normal FFPE controls using significance analysis of microarray (SAM) [18] (see Supporting information, Supplementary methods).

To further understand the functional and biological relevance of differentially expressed genes, gene ontology and pathway/network analysis was performed using the web-based software MetaCore (GeneGo, St Joseph, MI, USA). The software contains an interactive, manually annotated database derived from literature publications on proteins and small molecules that allows for representation of biological functionality and integration of functional, molecular, and clinical information. Several algorithms to enable both the construction and the analysis of gene networks were integrated as previously described [19]. The output p values reflect scoring, prioritization, and statistical significance of networks according to the relevance of input data.

Quantitative PCR for validation of selected genes

A reverse transcription reaction was carried out using the High Capacity cDNA Reverse Transcription Kit system (ABI, Foster City, CA, USA). Real-time fluorescent monitoring of the PCR products was performed using the Power SYBR Green PCR Master Mix (ABI) and gene-specific primers (Supporting information, Supplementary Table 4). Real-time PCR was performed in the ABI PRISM 7300 Sequence Detection system (Applied Biosystems, foster city, CA, USA) and analysed utilizing Sequence Detection Software v1.4 (ABI). Using endogenous GAPDH as an internal control for comparison, relative quantification of gene expression levels was performed and calculated using $2(-\Delta\Delta CT)$.

FISH for c-Myc translocation

MYC breakapart (BAP) probes were designed using the University of California Santa Cruz Genome Browser (http://www.genome.UCSC.edu) to identify bacterial artificial chromosomes (BACs) flanking the genes of interest (Supporting information, Supplementary Table 5). DNA was isolated (Plasmid Maxi Kit; Qiagen, Valencia, CA, USA) from BAC clones (ResGen™; Invitrogen, Carlsbad, CA, USA) and labelled with Texas Red-dUTP (Molecular Probes, Invitrogen, Carlsbad, CA, USA) or SpectrumGreen-dUTP (Abbott Molecular, Des Plaines, IL, USA). FISH was performed on TMA sections and scored as previously described [20]. Sections were analysed qualitatively by a microscopist (ML) and a minimum of 50 cells with strong FISH signals was required for a sample to be considered informative.

Terameprocol (EM-1421) treatment of NK cell lines

NK cell lines were treated with varying concentrations of the BIRC5 inhibitor Terameprocol (EM-1421; Erimos Pharmaceuticals, Houston, TX, USA) [21, 22] and control. Following incubation for 48 h, the cells were harvested, washed in PBS, and subjected to (i) MTS assay to evaluate the degree of cell viability (see Supporting information, Supplementary methods); (ii) flow cytometric analysis to assess the degree of apoptotic cell death using Annexin-V-APC and propidium iodide (PI) staining (BD Pharmigen, CA, USA); and (iii) western blot analysis to confirm successful inhibition of BIRC5 (Supporting information, Supplementary methods). The flow cytometry analysis was performed on a BD LSR II flow cytometer (Becton Dickinson, CA, USA) using BD FACSDiva™ software.

Table 1. Pathways and cellular processes enriched in genes differentially expressed between NKTL and normal NK cells

Map	Map folders	Cell process	*p* value	Objects in gene list	Objects in map
Cell cycle_The metaphase checkpoint	Congenital, Hereditary, and Neonatal Diseases and Abnormalities Regulatory processes/Cell cycle	Cell cycle	4.01E-05	10	36
Cell cycle_Chromosome condensation in prometaphase	Regulatory processes/Cell cycle	Cell cycle	1.21E-04	7	20
Cell cycle_Transition and termination of DNA replication	Regulatory processes/Cell cycle	Cell cycle	7.48E-04	7	26
Cell cycle_Start of DNA replication in early S phase	Regulatory processes/Cell cycle	Cell cycle	2.30E-03	7	31
Cell cycle_Role of APC in cell cycle regulation	Regulatory processes/Cell cycle	Cell cycle	2.79E-03	7	32
Cell cycle_Initiation of mitosis	Congenital, Hereditary, and Neonatal Diseases and Abnormalities Regulatory processes/Cell cycle	Cell cycle	3.42E-03	6	25
Cell cycle_Spindle assembly and chromosome separation	Regulatory processes/Cell cycle	Cell cycle	1.22E-02	6	32
DNA damage_ATM/ATR regulation of G2/M checkpoint	Congenital, Hereditary, and Neonatal Diseases and Abnormalities Regulatory processes/Cell cycle Regulatory processes/DNA damage	Cell cycle	1.96E-02	5	26
Transcription_Sin3 and NuRD in transcription regulation	Regulatory processes/Transcription	Transcription	2.73E-02	6	38
Cell cycle_Cell cycle (generic schema)	Congenital, Hereditary, and Neonatal Diseases and Abnormalities Regulatory processes/Cell cycle	Cell cycle	3.72E-02	4	21
Development_MAG-dependent inhibition of neurite outgrowth	Congenital, Hereditary, and Neonatal Diseases and Abnormalities Protein function/Growth factors Regulatory processes/Development/Neurogenesis	Intracellular receptor-mediated signalling pathway, response to extracellular stimulus	4.44E-02	5	32

Results

Analysis of GEP of NKTL

We compared the gene expression of NKTL FFPE samples ($n = 9$) with that of normal NK cells, as well as the respective normal FFPE tissue controls from nasal, skin and soft tissue, intestinal tract, and lymph node (see Supporting information, Supplementary methods). Among the genes showing at least a two-fold and statistically significant difference ($p < 0.05$), 339 were found to be up-regulated and 737 were down-regulated in NKTL compared with normal NK cells (Supporting information, Supplementary Table 6). We performed quantitative PCR validation on a few interesting genes frequently involved in tumour oncogenesis, including *BIRC5* (*survivin*), *EZH2*, *STMN1*, and *WHSC1*. On the whole, the quantitative PCR results were consistent with GEP data showing overexpression of *BIRC5*, *EZH2*, and *STMN1* in NK cell lines compared with normal NK cells (see the Supporting information, Supplementary Figure 1).

These differentially expressed genes were significantly enriched for cell cycle-related pathways and processes (Table 1), suggesting that NKTLs are significantly more proliferative than normal NK cells. Amongst the key proteins involved in cell cycle and mitosis are PLK1, CDK1, and Aurora-A. These proteins may also be potential therapeutic targets because of their involvement in carcinogenesis [23–25].

Using MetaCore, we found that the differentially expressed genes between NKTL and normal NK cells were enriched for targets of a number of transcription factors including Myc, p53, and NF-κB subunits (Table 2). When we further examined the expression of the Myc transcription targets and their relationship with Myc, it was striking that most of the genes up-regulated and down-regulated in our list of differentially expressed genes have been shown by previous experiments to be concordantly expressed and repressed by Myc (Figure 1A). This result suggests that Myc is activated in NKTL compared with normal NK cells. In contrast, the transcription targets of p53 in our list of differentially expressed genes showed a predominantly opposite effect to what is expected under normal p53 control, ie genes that are normally repressed by p53 were up-regulated in NKTL compared with normal NK cells, and vice versa (Figure 1B), indicating deregulation of the p53 transcription factor in NKTL compared with normal NK cells.

We further assessed the expression of a previously published NF-κB signature [26] and a validated MYC signature (unpublished) in the gene expression dataset.

Table 2. Targets of transcription targets enriched amongst genes differentially expressed between NKTL and normal NK cells

No	Network	GO processes	Total nodes	Root nodes	*p* value	zScore	gScore
1	c-Myc	Cell cycle (33.8%; 4.867e-13), cell division (21.1%; 2.325e-12), cell cycle process (26.8%; 4.968e-11), cell cycle phase (23.9%; 5.019e-11), mitotic cell cycle (21.1%; 5.843e-10)	73	72	3.28E-149	89.37	89.37
2	SP1	Cell division (13.8%; 2.728e-06), positive regulation of cellular process (35.4%; 3.296e-06), positive regulation of catalytic activity (18.5%; 4.041e-06), regulation of catalytic activity (23.1%; 4.731e-06), regulation of molecular function (24.6%; 4.773e-06)	65	64	2.66E-132	84.18	84.18
3	p53	Regulation of cell cycle (26.7%; 3.272e-11), cell cycle (33.3%; 5.758e-11), cell division (20.0%; 7.506e-10), cell cycle process (26.7%; 1.779e-09), cell cycle checkpoint (13.3%; 2.766e-09)	62	61	5.59E-126	82.15	82.15
4	ESR1 (nuclear)	Regulation of cell cycle (25.0%; 2.165e-08), cell division (18.8%; 1.881e-07), cell cycle checkpoint (12.5%; 4.328e-07), regulation of mitotic cell cycle (14.6%; 6.202e-07), negative regulation of cellular process (39.6%; 1.318e-06)	53	52	4.48E-107	75.73	75.73
5	CREB1	Cell cycle (31.7%; 2.639e-07), M phase (22.0%; 3.244e-07), regulation of cell cycle (24.4%; 4.238e-07), cell division (19.5%; 6.635e-07), cell cycle phase (22.0%; 4.111e-06)	42	41	4.25E-84	67.07	67.07
6	RelA (p65 NF-κB subunit)	Regulation of cell proliferation (38.9%; 2.214e-08), positive regulation of biological process (52.8%; 6.173e-08), developmental process (69.4%; 8.591e-08), biological regulation (94.4%; 8.778e-08), positive regulation of cellular process (50.0%; 8.804e-08)	38	37	8.86E-76	63.63	63.63
7	GATA-1	Cell division (22.9%; 1.798e-07), regulation of cell cycle (25.7%; 9.966e-07), M phase (22.9%; 1.068e-06), cell cycle checkpoint (14.3%; 2.108e-06), cell cycle (31.4%; 2.446e-06)	35	34	1.49E-69	60.92	60.92
8	Androgen receptor	Regulation of cell cycle (33.3%; 1.553e-08), M phase (30.0%; 1.661e-08), cell cycle (40.0%; 3.930e-08), cell division (26.7%; 4.844e-08), negative regulation of cellular process (53.3%; 5.874e-08)	33	32	2.07E-65	59.04	59.04
9	c-Fos	Biological regulation (93.8%; 8.492e-07), regulation of metabolic process (62.5%; 2.756e-06), regulation of cellular process (87.5%; 4.280e-06), regulation of cell cycle (25.0%; 5.084e-06), M phase (21.9%; 7.025e-06)	32	31	2.44E-63	58.09	58.09
10	c-Rel (NF-κB subunit)	Regulation of cell cycle (31.0%; 1.674e-07), cell cycle (34.5%; 2.717e-06), M phase (24.1%; 3.459e-06), mitotic cell cycle (24.1%; 9.697e-06), cell division (20.7%; 1.212e-05)	31	30	2.85E-61	57.11	57.11
11	HNF6	Regulation of cell cycle (31.0%; 1.674e-07), M phase (27.6%; 2.200e-07), cell cycle (37.9%; 2.788e-07), cell division (24.1%; 7.233e-07), mitotic cell cycle (27.6%; 7.253e-07)	30	29	3.33E-59	56.12	56.12
12	PPAR-gamma	Regulation of cell cycle (31.0%; 1.674e-07), cell cycle (37.9%; 2.788e-07), cell division (24.1%; 7.233e-07), mitotic cell cycle (27.6%; 7.253e-07), cell cycle checkpoint (17.2%; 7.936e-07)	29	28	3.87E-57	55.11	55.11
13	STAT3	M phase (27.6%; 2.200e-07), cell cycle (37.9%; 2.788e-07), cell division (24.1%; 7.233e-07), mitotic cell cycle (27.6%; 7.253e-07), cell cycle process (31.0%; 1.649e-06)	29	28	3.87E-57	55.11	55.11
14	E2F1	Cell division (42.9%; 2.758e-14), cell cycle (57.1%; 1.936e-13), mitotic cell cycle (42.9%; 2.870e-12), cell cycle phase (42.9%; 1.646e-11), DNA metabolic process (42.9%; 3.985e-11)	28	27	4.49E-55	54.08	54.08
15	HIF1A	Regulation of cell cycle (37.0%; 4.751e-09), negative regulation of cellular process (55.6%; 7.431e-08), cell cycle (40.7%; 1.168e-07), negative regulation of biological process (55.6%; 2.183e-07), regulation of mitotic cell cycle (22.2%; 2.953e-07)	27	26	5.19E-53	53.03	53.03
16	CDP/Cux	Cell cycle (59.3%; 8.763e-14), M phase (37.0%; 2.405e-10), mitotic cell cycle (37.0%; 1.107e-09), mitosis (29.6%; 2.891e-09), M phase of mitotic cell cycle (29.6%; 3.407e-09)	27	26	5.19E-53	53.03	53.03

Table 2. (*Continued*)

No	Network	GO processes	Total nodes	Root nodes	*p* value	zScore	gScore
17	N-Myc	Cell cycle (46.2%; 5.436e-09), cell division (30.8%; 1.378e-08), regulation of cell cycle (34.6%; 5.685e-08), mitotic cell cycle (30.8%; 2.836e-07), cell cycle checkpoint (19.2%; 4.460e-07)	26	25	5.97E-51	51.96	51.96
18	GCR-alpha	Negative regulation of cellular process (57.7%; 3.722e-08), negative regulation of biological process (57.7%; 1.105e-07), cell division (26.9%; 3.196e-07), cell cycle (38.5%; 8.437e-07), regulation of cell cycle (30.8%; 8.926e-07)	26	25	5.97E-51	51.96	51.96
19	AML1 (RUNX1)	Regulation of cell cycle (38.5%; 3.078e-09), cell cycle (46.2%; 5.436e-09), cell division (30.8%; 1.378e-08), mitotic cell cycle (34.6%; 1.544e-08), cell cycle process (38.5%; 4.140e-08)	26	25	5.97E-51	51.96	51.96
20	TCF7L2 (TCF4)	Negative regulation of cellular process (60.0%; 1.775e-08), regulation of cell cycle (36.0%; 3.824e-08), cell cycle (44.0%; 4.443e-08), negative regulation of biological process (60.0%; 5.327e-08), cell cycle process (36.0%; 3.906e-07)	25	24	6.85E-49	50.87	50.87
21	VDR	Cell division (28.0%; 2.373e-07), cell cycle (40.0%; 5.473e-07), regulation of cell cycle (32.0%; 6.354e-07), M phase (28.0%; 1.154e-06), mitotic cell cycle (28.0%; 3.281e-06)	25	24	6.85E-49	50.87	50.87
22	ATF-2	Cell cycle (40.0%; 5.473e-07), regulation of cell cycle (32.0%; 6.354e-07), M phase (28.0%; 1.154e-06), mitotic cell cycle (28.0%; 3.281e-06), cell division (24.0%; 4.806e-06)	25	24	6.85E-49	50.87	50.87
23	IRF1	Regulation of cell cycle (36.0%; 3.824e-08), cell cycle (40.0%; 5.473e-07), M phase (28.0%; 1.154e-06), mitotic cell cycle (28.0%; 3.281e-06), cell division (24.0%; 4.806e-06)	25	24	6.85E-49	50.87	50.87
24	FKHR	Cell cycle (41.7%; 3.461e-07), regulation of cell cycle (33.3%; 4.443e-07), negative regulation of cellular process (54.2%; 8.335e-07), M phase (29.2%; 8.479e-07), post-translational protein modification (45.8%; 1.468e-06)	24	23	7.83E-47	49.75	49.75
25	Brca1	Regulation of cell cycle (41.7%; 1.203e-09), cell cycle (50.0%; 1.694e-09), cell cycle checkpoint (25.0%; 5.340e-09), cell cycle process (41.7%; 1.649e-08), mitotic cell cycle (33.3%; 1.401e-07)	24	23	7.83E-47	49.75	49.75
26	RARalpha	Cell division (29.2%; 1.736e-07), cell cycle (41.7%; 3.461e-07), regulation of cell cycle (33.3%; 4.443e-07), negative regulation of cellular process (54.2%; 8.335e-07), M phase (29.2%; 8.479e-07)	24	23	7.83E-47	49.75	49.75
27	MYOD	Cell cycle (41.7%; 3.461e-07), regulation of cell cycle (33.3%; 4.443e-07), M phase (29.2%; 8.479e-07), cell differentiation (54.2%; 1.202e-06), post-translational protein modification (45.8%; 1.468e-06)	24	23	7.83E-47	49.75	49.75
28	HMGI/Y	Cell cycle (43.5%; 2.128e-07), regulation of cell cycle (34.8%; 3.046e-07), M phase (30.4%; 6.128e-07), mitotic cell cycle (30.4%; 1.754e-06), cell cycle process (34.8%; 2.387e-06)	23	22	8.91E-45	48.61	48.61
29	HOXD13	Cell division (30.4%; 1.249e-07), cell cycle (43.5%; 2.128e-07), regulation of cell cycle (34.8%; 3.046e-07), M phase (30.4%; 6.128e-07), regulation of cell proliferation (43.5%; 6.871e-07)	23	22	8.91E-45	48.61	48.61
30	PPARGC1 (PGC1-alpha)	Cell cycle (43.5%; 2.128e-07), regulation of cell cycle (34.8%; 3.046e-07), M phase (30.4%; 6.128e-07), mitotic cell cycle (30.4%; 1.754e-06), cellular biopolymer metabolic process (87.0%; 1.992e-06)	23	22	8.91E-45	48.61	48.61

Consistent with the MetaCore analysis, we observed that the MYC and NF-κB signatures were highly expressed in the NK cell lines and tumour samples compared with normal NK cells. When these two signatures were summarized into indices using the median expression of genes constituting the respective signatures, both the NF-κB index and the MYC index were significantly higher in NK cell lines and NKTL than in normal NK cells (Figure 1C).

As NKTL is an aggressive lymphoma often with extranodal involvement, we wanted to see if there was any enrichment among dysregulated genes for cell

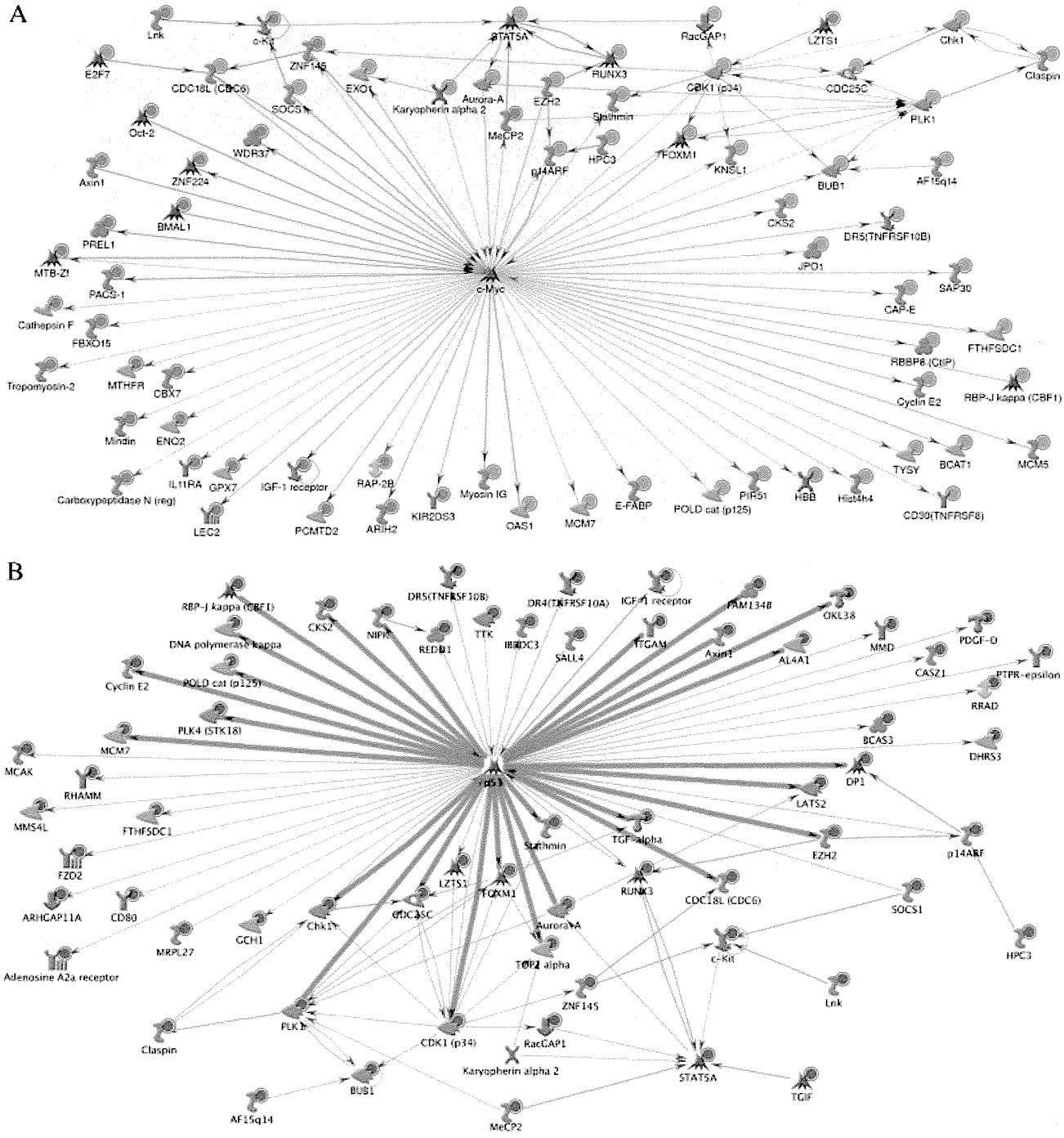

Figure 1. Gene expression profiling and networks formed by genes differentially expressed between NKTL and normal NK cells as analysed using MetaCore. (A) Network comprising transcriptional targets of MYC. Most of the transcriptional targets are expressed in concordance with the expected effect of MYC activation. (B) On the other hand, expression of transcriptional targets of p53 is discordant with the expected effect of p53 activated (interactions highlighted by magenta colour). In these figures, genes in our differentially expressed gene list (Supporting information, Supplementary Table 6) are indicated by a red circular 'target' or a blue circular 'target' to the upper right of the gene symbols if overexpressed or underexpressed, respectively. The directions of arrows connecting different molecules indicate the direction of interaction. Connecting lines in green represent a stimulating interaction and those in red an inhibitory interaction. If the line is in grey, the nature of the interaction is unknown. The different symbols signify different functions of each molecule, eg transcription factors, receptors, etc. (C) Heat map showing expression of NF-κB and MYC signatures in NK cell lines, NKTL and normal NK cells, and tissue control. Overexpressed and underexpressed genes are in red and green, respectively, with yellow indicating median expression. The dot-plot indicates that when these signatures are summarized into indices, both the NFKB and the MYC indices are significantly higher in NK cell lines and NKTL than in normal NK cells.

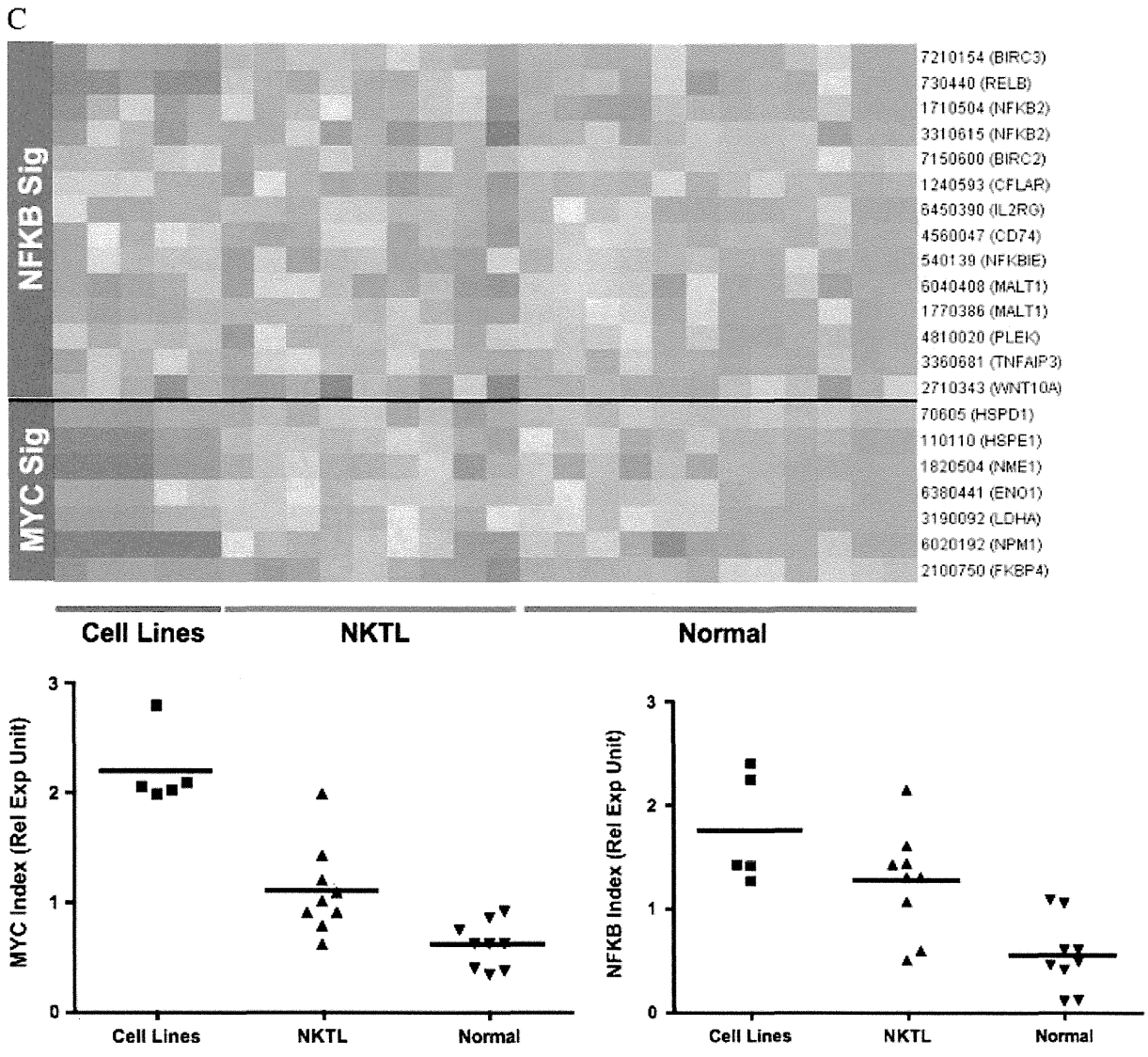

Figure 1. (*Continued*).

adhesion or metastasis-related genes. We performed Individual Pathway Activity Score Analysis (iPASA, http://lab.selfip.net/iPASA/) [27], a modification of gene set enrichment analysis, and found several metastasis-related gene sets to have higher scores in NKTL and NK cell lines than in normal NK cells (Supporting information, Supplementary Figure 2). However, an analysis of the genes contributing most significantly to the high scores of these gene sets suggested that this was predominantly due to cell cycle-related genes (Supporting information, Supplementary Figure 3).

Immunohistochemistry

To validate our gene expression results, we performed IHC for c-Myc, p53, all five subunits of the NF-κB pathway, and survivin on TMA sections containing 33 samples of NKTL. In corroboration with the GEP findings, we observed a significant percentage of our NKTL cases showing positive expression for c-Myc (15/33, 45.4%), p53 (29/33, 87.9%), NF-κB p50 (21/31, 67.7%), and survivin (32/33, 97%) (Figure 2 and Supporting information, Supplementary Table 7). Furthermore, there was a significant correlation between c-Myc immunoreactivity and the

Figure 2. Validation of gene expression profiling by IHC. (A, B) Case NKTL 23 showing nuclear expression of c-Myc in the medium and large tumour cells. (A) H&E (B) c-Myc. (C, D) Case NKTL 33 showing strong p53 nuclear staining in the neoplastic cells, which range from small to large and display irregular nuclear contours. (C) H&E (D) p53. (E, F) Strong nuclear expression for survivin observed in the medium and large neoplastic lymphocytes in case NKTL 32. (E) H&E (F) survivin. (G, H) Case NKTL 9 with positive nuclear and cytoplasmic staining for p50 in the small neoplastic lymphocytes. Only nuclear expression is regarded as constitutive p50 activation. (G) H&E (H) p50. (I, J) Moderate to strong nuclear and cytoplasmic immunoreactivity for RelB in the large pleomorphic lymphoid cells of case NKTL 6. (I) H&E (J) RelB. All photographs were taken with a DP20 Olympus camera (Olympus, Tokyo, Japan) using an Olympus BX41 microscope (Olympus). Images were acquired using DP Controller 2002 (Olympus) and processed using Adobe Photoshop version 5.5 (Adobe Systems, San Jose, CA, USA). Original magnifications: ×600 (A–J).

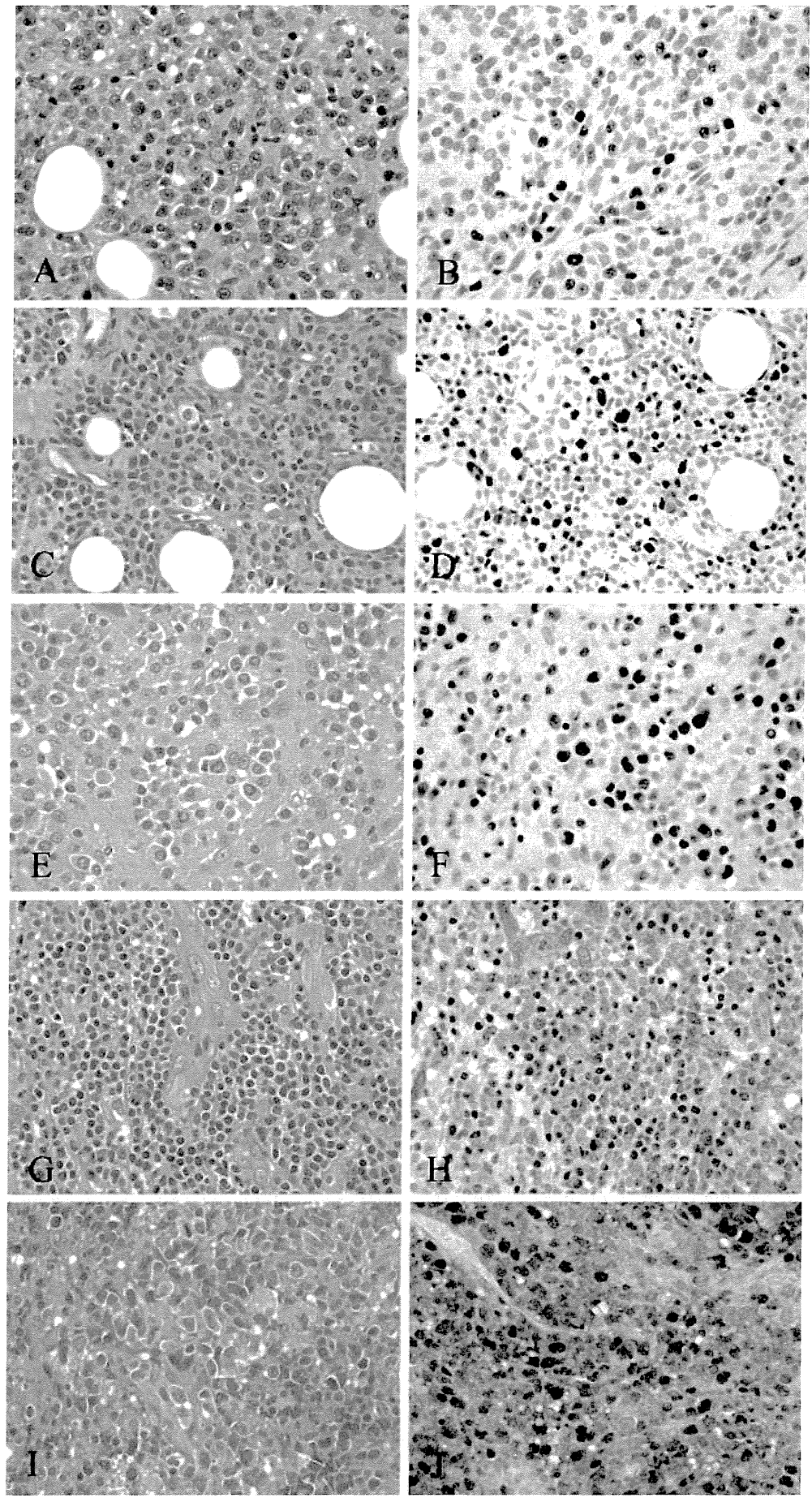

Figure 2.

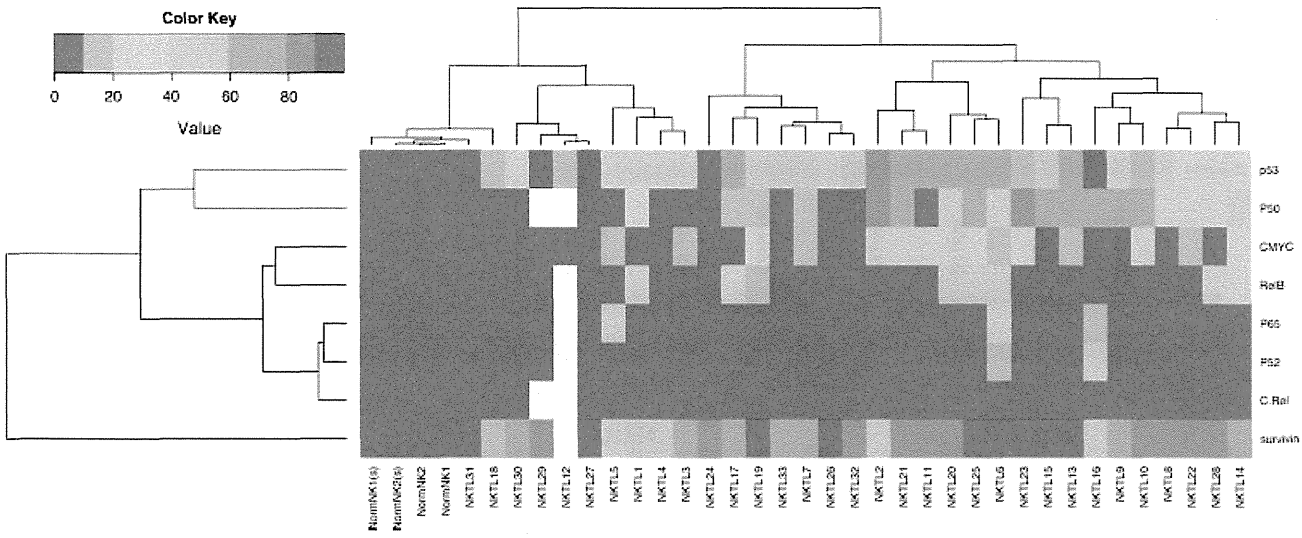

Figure 3. Clustering of samples based on expression of markers on IHC in NKTL (heat map). The samples used for IHC analysis were clustered based on the percentage of cells expressing the different markers used for IHC. Almost all cases of NKTL expressed aberrant p53 and survivin (not expressed in normal NK cells). Two main groups of NKTLs are defined by the expression pattern of these markers, with one group having c-Myc expression and stronger p50 expression, whereas the other only occasionally expresses c-Myc and p50. The legend for the colour coding in the heat map is shown to the upper left of the figure. 'White' indicates that tissue was not available for IHC staining of these markers.

MYC index (Supporting information, Supplementary Figure 4). Using FISH analysis, no break-apart signals were observed in 12 cases with adequate tumour cells and adequate hybridization, suggesting that MYC activation is not due to MYC rearrangements. In addition to p50, which is involved in the canonical NF-κB pathway, 27.3% (9 of 33) of NKTLs demonstrated positive expression for RelB, indicating that the non-canonical pathway may also be activated in a subset of NKTLs. In contrast, p52 and p65 were only infrequently expressed in 2 of 32 and 3 of 32 cases, respectively. None of our cases expressed c-Rel. Particularly striking was the immunoreactivity for survivin, where 29 out of the 32 positive cases (91%) showed expression in 50% or more of the tumour cell population, with strong staining in the majority of the cases. As expected, normal NK cells showed no expression or less than 10% expression for all the antibodies (Supporting information, Supplementary Table 8).

In order to study the relationship between the activation of Myc, p53, and NF-κB pathways and to determine whether there are distinct clusters based on the combination of these pathways, we clustered the samples according to the level of immunoreactivity for the different antigens (Figure 3). Almost all samples overexpressed p53 and survivin. Two main clusters were observed. The first, with hardly any expression of the markers tested, was clustered together with the normal NK cell samples. The second large cluster contained the remaining samples, with aberrant expression of one or more of these markers. Within the second cluster were two sub-clusters, one showing higher expression of p50 and c-Myc compared with the other. The clinical relevance of the different patterns of expression of these markers is not known as our sample size was small and there was no apparent difference in survival between these groups when we correlated the data with clinical outcome (data not shown).

Inhibition of survivin leads to apoptosis in NKTL cell lines

As survivin was aberrantly expressed in most of the NKTLs, we investigated whether inhibition of survivin would be therapeutically useful. We used western blot to assess the level of survivin protein expression in five NK cell lines (KHYG-1, NK-92, NK-YS, HANK-1, and SNK-6) and found overexpression of survivin in NK cell lines compared with normal NK cells, consistent with the IHC results (Figure 4A). The three cell lines with the highest survivin expression (KHYG-1, NK-92, and SNK-6) were selected for treatment with Terameprocol (EM-1421), a survivin inhibitor [21,22]. Successful suppression of survivin confirmed by western blot (Figure 4B) in KHYG-1 and NK92 resulted in a significant decrease in cell viability using the MTS assay (Figure 4C) and a dose-dependent increase in apoptosis compared with the control, as demonstrated in the bar chart (Figure 4D). In contrast, no significant change in cell viability or apoptosis in SNK-6 was observed when survivin was not suppressed by the inhibitor.

Discussion

NKTL is a relatively rare lymphoma that is highly aggressive, and current treatment strategies are clearly sub-optimal and chemoresistance is common [8,28]. A better understanding of the molecular abnormalities underlying this condition will provide important insights into the biology of this disease. In the past,

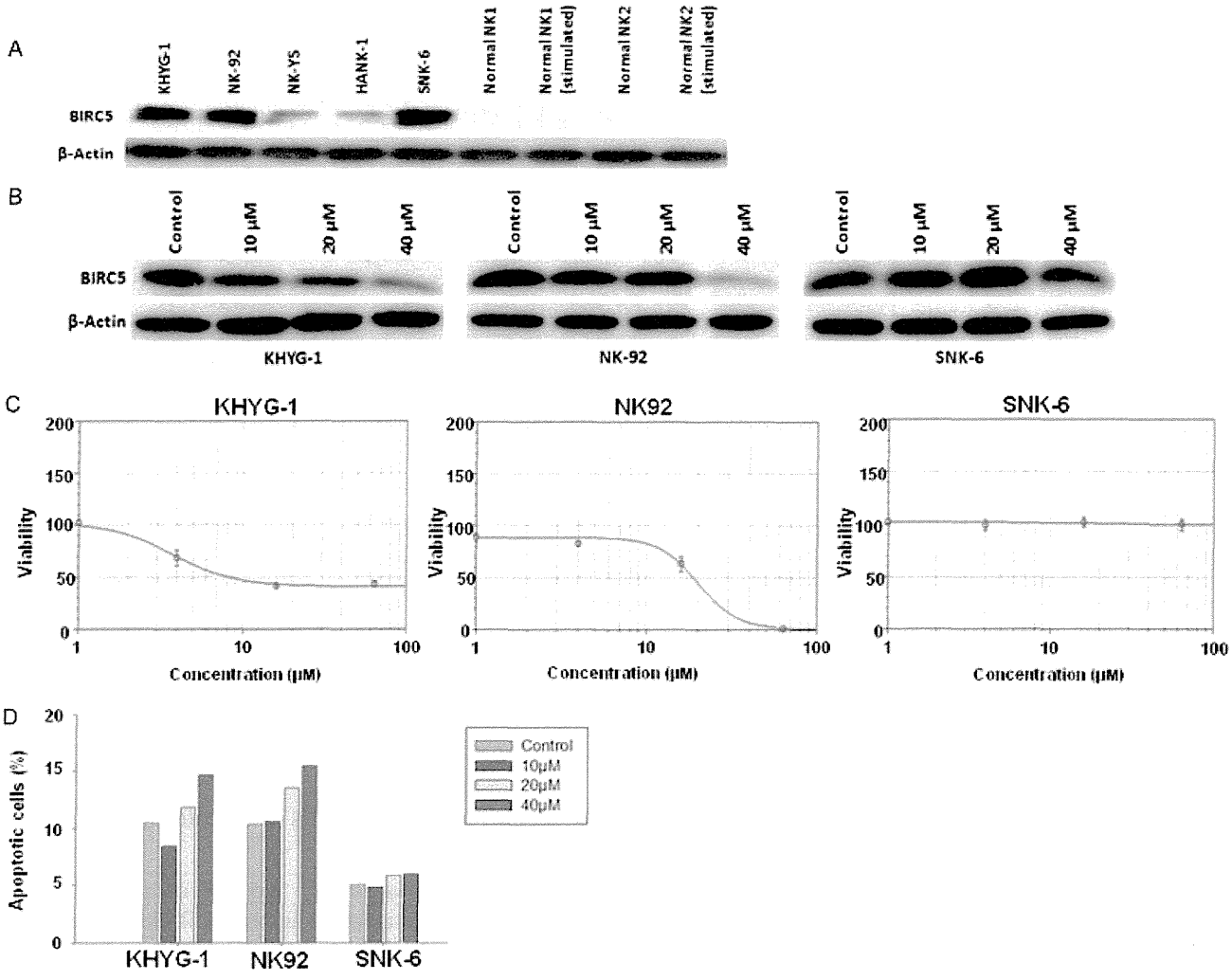

Figure 4. Inhibition of survivin leads to apoptosis in NK cell lines. Three NK cell lines with high expression of survivin (KHYG-1, NK-92, and SNK-6) identified by western blot (A) were treated with Terameprocol (survivin inhibitor) at 10, 20, and 40 μM or control for 48 h. There was successful dose-dependent inhibition of survivin in KHYG-1 and NK-92, confirmed by western blot with β-actin as the loading control (B). This was accompanied by a decrease in more than 50% of cell viability in the two cell lines and an increase in apoptosis detected by flow cytometry (C, D). The different concentrations of Terameprocol are represented by different colours according to the colour legend on the upper right of figure D. In contrast, there was no significant increase in apoptosis or decrease in cell viability in SNK-6 when survivin was not suppressed by the inhibitor.

it has been impossible to perform GEP using FFPE, due to RNA fragmentation. However, recent technology has enabled good-quality gene expression data to be obtained from FFPE samples [12]. We have shown in our study using a similar platform that we can obtain useful and meaningful GEP results from FFPE tissue. The validity of our results was supported by quantitative PCR validation as well as corroboration of our in silico functional analysis with immunohistochemistry in a larger TMA dataset, showing a good correlation between GEP, IHC, and western blot results. We did not attempt to categorize our cases into different clinical subtypes according to the site of involvement or cell of origin because of the small sample size.

Our results demonstrate a pro-proliferative and anti-apoptotic phenotype in NKTL, compared with normal NK cells, which is characterized by the activation of Myc and NF-κB, and deregulation of p53. NF-κB transcription factors are key regulators of immune, inflammatory, and acute phase responses [29] that have been implicated in oncogenesis through their transcription regulation of genes involved in cell cycle proliferation and cell adhesion, inhibition of apoptosis (including survivin) [30], and induction of cancer treatment resistance via the expression of multi-drug resistance-1 in tumour cells [30]. Among lymphoid malignancies, activation of NF-κB has been reported in mycosis fungoides [31], classical Hodgkin lymphoma, anaplastic large cell lymphoma, and peripheral T-cell lymphoma [32]. In NKTL, Liu *et al* [13] observed activation of NF-κB through the non-canonical pathway in 65.2% of NKTLs in China, and these cases were associated with chemoresistance and poor prognosis. NF-κB activation has also been shown in NK cell lines, and treatment of tumour cells with NF-κB inhibitors (BAY 11–7082 and curcumin) resulted in the suppression of NF-κB activation and induction of apoptosis [33]. Our data indicate